Temporal shaping of high-voltage picosecond electric pulses for electronic spectroscopy and bioelectric applications

Sahar Wehbi, Nour Tabcheh, Alessandro Tonello, Rosa Orlacchio, Philippe Lévêque, Delia Arnaud-Cormos, Tigran Mansuryan, Marc Fabert, Olivier Tantot, Sebastien Vergnole, et al.

MICROWAVE AND OPTICAL TECHNOLOGY LETTERS

Temporal Shaping of High-Voltage Picosecond Electric Pulses for Electronic Spectroscopy and Bioelectric Applications

Journal:	*Microwave and Optical Technology Letters*
Manuscript ID	MOP-22-1016
Wiley - Manuscript type:	Research Article
Date Submitted by the Author:	29-Sep-2022
Complete List of Authors:	Arnaud-Cormos, Delia; Universite de Limoges Faculte des Sciences et Techniques; Institut Universitaire de France Wehbi, Sahar; Universite de Limoges Faculte des Sciences et Techniques Tabcheh, Nour; Universite de Limoges Faculte des Sciences et Techniques Tonello, Alessandro; Universite de Limoges Faculte des Sciences et Techniques Orlacchio, Rosa; Universite de Limoges Faculte des Sciences et Techniques LEVEQUE, philippe; Universite de Limoges Faculte des Sciences et Techniques Mansuryan, Tigran; Universite de Limoges Faculte des Sciences et Techniques Fabert, Marc; Universite de Limoges Faculte des Sciences et Techniques Tantot, Olivier; Universite de Limoges Faculte des Sciences et Techniques Vergnole, Sebastien; ALPhANOV Centre Technologique Optique et Lasers Couderc, Vincent; Universite de Limoges Faculte des Sciences et Techniques
Keywords:	Electronic spectroscopy, optoelectronic devices, optoelectronic switching, temporal shaping photoconductivity switching

Temporal Shaping of High-Voltage Picosecond Electric Pulses for Electronic Spectroscopy and Bioelectric Applications

Sahar Wehbi[1], Nour Tabcheh[1], Alessandro Tonello[1], Rosa Orlacchio[1], Philippe Leveque[1], Delia Arnaud-Cormos[1,2], Tigran Mansuryan[1], Marc Fabert[1], Olivier Tantot[1], Sebastien Vergnole[3], and Vincent Couderc[1]

[1] University of Limoges, CNRS, XLIM, UMR 7252, F-87000 Limoges, France
[2]Institut Universitaire de France (IUF), 75005 Paris, France
[3]ALPhANOV, Optics & Lasers Technology Center, Institut d'optique d'Aquitaine, Rue François Mitterrand, 33400 Talence, France

Corresponding author
Vincent COUDERC
Email: vincent.couderc@unilim.fr

Running title
Electric pulses for electronic spectroscopy

Abstract
In this paper, we present temporal and spectral shaping of kilovolt picosecond electrical pulses obtained by using the linear switching process with femtosecond laser source. The frozen wave generator integrating up to four photoconductive semi-conductor switches is activated by varying the optical pulse amplitude and time delay. Electric pulses with rise time and duration as short as 60 ps and 100 ps, respectively are used to implement a microwave spectroscopy experiment. This optoelectronic device is synchronous with the optical pulses which can be used for optical spectroscopy, after nonlinear frequency conversion. This single-shot microwave spectroscopy technique was used to characterize resonances of a passive dielectric resonator. Pulse shaping integrating coherent wave combining is also demonstrated.

Keywords
Electronic spectroscopy, optoelectronic devices, optoelectronic switching, temporal shaping photoconductivity switching.

I. INTRODUCTION

Ultrashort high intensity pulsed electric fields (PEFs) can elicit different bioeffects. PEF with durations shorter than the plasma membrane charging time (~ 100 ns) and strengths of ~ MV/m can affect intracellular structures [1], [2]. Biological effects of ultrashort pulses gained interest in the last two decades with the development of generators providing controlled pulses [3]–[8]. Maintaining kilovolt pulses while decreasing their duration is a challenging task especially when a temporal synchronization with an optical imaging system is required. Ultrafast optoelectronic switches integrated in microstrip or coaxial transmission lines triggered by a laser beam were recently used for ultrashort pulses generation. Photoconductive semiconductor switches (PCSSs) operating in a linear switching regime allow the generation of nanosecond or subnanosecond electric pulses without any temporal jitter with respect to the optical pulses used for their activation [9]–[12].

Fast imaging methods like Multiplex Coherent Anti-Stokes Raman Scattering (M-CARS) were used to study the interaction between PEF and cells. The nanosecond temporal resolution [13]–[15] of these methods is within the range of biological samples time response as suggested by molecular dynamics simulations [16], [17].

To further contribute to the study of dynamic biological phenomena requiring ultrashort temporal resolution following picosecond PEF (psPEF) exposure, we designed and characterized an ultrashort electric pulses generator (down to 60 ps). The generator is based on the frozen wave (FW) concept [12] and synchronized with an ultrafast microwave spectroscopy system able to determine the resonances of a passive resonator placed in an electromagnetic waveguide i.e., a transverse electromagnetic (TEM) cell [18].

II. EXPERIMENTAL SETUP

A. Optoelectronic Generator

Our FW generator [9]–[11] implemented two PCSSs connected on both ends of a 50-Ω microstrip transmission line (Fig. 1). To double the voltage sustaining the switches, two identical PCSSs can be connected in series. The circuit was terminated by a second line connected to the ground while its input is connected to a 70 GHz bandwidth oscilloscope (DPO70000SX, Tektronix) through an 86 dB attenuation chain. The PCSSs are silicon semiconductors (GP02-40, Vishay) sustaining up to 4 kV in static configuration. A DC high voltage source was connected to the transmission line allowing its DC energy charging. PCSSs were triggered by a high energy laser (Tangerine HP, Amplitude system) which beam energy, repetition rate, and duration can be tuned between 0 and 250 µJ, 0 and 40 MHz, and 350 fs and 10 ps, respectively. The electric pulse duration is imposed by the length of the transmission line separating the two pairs of PCSSs, i.e., 2- or 20-mm lines. PCSSs were used in their linear regime for perfect combination of all four instantaneous responses with no temporal jitter between optical and electrical pulses. Four half-

waveplates along with beam splitters allowed to control the amount of energy illuminating the PCSSs. Optical delay lines were used to define PCSSs switching times and amount of energy released. Unipolar, bipolar, or successive unipolar pulses were generated.

B. Microwave Spectroscopy

Ultrashort pulses with a large frequency spectrum were implemented to acquire fast responses of exposed samples, microwave resonances and properties [19], [20]. The microwave spectroscopy setup is schematically represented on Fig. 1. A TEM cell was used to deliver the unipolar psPEF to a cylindric dielectric resonator (E2000, Exxelia Temex) accommodated within the TEM cell in contact with the central plate (Fig. 2). TEM cells are open propagating devices able to maintain a homogeneous electric field distribution on a large transverse dimension (10 cm). For spectroscopy measurements, a single 105 ps unipolar PEF with a frequency spectrum covering 7.5 GHz at –20 dB was used. The resonator locally modifies the impedance and propagation in the TEM cell depending on the frequency spectrum. The modified signal was acquired with the oscilloscope connected to the TEM cell output (Fig.1). To analyze the resonances introduced by the passive resonator, a Fourier transform was performed on the output signal. Results were compared to the scattering S-parameters (S_{21}) of the structure measured within the 10 kHz – 5 GHz frequency range through a vector network analyser (ZVA24, Rohde&Schwarz).

III. NUMERICAL SIMULATIONS

A numerical characterization of the microwave spectroscopy system was performed using CST Microwave Studio 2020 (Dassault Systems). The TEM cell was modelled as shown in Fig. 2. Each metallic plate was 1 mm thick. The dielectric resonator was modelled with a relative permittivity and a loss tangent of 37 and 0.02, respectively, while perfect electrical conductors (PEC) was used for the metallic components. 50-Ohm waveguide ports modelled the feeding source/load at the TEM cell input/output. Simulations were performed between 0 and 5 GHz. For accuracy non-uniform adaptive meshing was implemented. The resonator was modelled with a grid mesh of 0.648 mm × 0.648 mm × 0.1 mm, while larger grid cells (3.95 mm × 3.54 mm × 0.1 mm) were applied to other parts of the structure.

IV. RESULTS AND DISCUSSION

A. Unipolar, bipolar, and successive unipolar pulses

Bipolar pulses were generated with two PCSSs connected by a 2-mm length transmission line. Fig. 3(a) and (b) show the temporal and spectral shaping of three pulses obtained for different commutation efficiencies of the two PCSSs. For a 4 kV input bias voltage and a 20 µJ optical energy, the synchronized illumination of the two PCSSs generates a bipolar pulse with a 1.6 kV peak-to-peak output voltage. The pulse total duration, measured at 10% of the rise and fall times, was equal to 333 ps with 53 ps peak-to-peak transition between the positive and the negative polarity. The pulse frequency spectrum considered at -20 dB level covers 7.8 GHz bandwidth. The pulse shape and output spectrum can be controlled by the time delay or the optical energy of the two laser beams illuminating the PCSSs. Triggering the second PCSS with less than 10 µJ significantly decreased the negative part of the pulse and therefore increased the lower frequency content in the spectrum profile (Fig. 3, pulses #1 and #2).

To generate two successive unipolar pulses separated by 500 ps, two PCSSs were connected by a 2-cm transmission line and three delay lines were implemented (Fig. 4(a)). The activation of PCSS1 with 10 µJ optical energy (F1a) generated a triangular pulse with several maxima (Fig. 4(b)) as the switching process was incomplete at this instant. The total pulse duration and rise time were 2 ns and 70 ps, respectively. After 500 ps, a 20 µJ fs optical pulse (F1b) illuminated again PCSS1 creating a second positive pulse delayed by 500 ps with respect to the first one. Observed alone, the second switching created a positive pulse with a peak voltage, rise time, and duration of 1.72 kV, 75 ps, and 450 ps, respectively (Fig. 4(c), 4 kV bias voltage). Finally, PCSS2 was activated by a 250-ps delayed fs optical pulse (F2) with 10 µJ energy. When

activating PCSS2 alone, a negative pulse of -250 V amplitude, 120-ps duration, and 75-ps rise time was generated (Fig. 4(d)). By coherent combination of F1a, F1b, and F2 with the associated optical delays, two successive positive pulses of 670 V were produced (Fig. 4(e)). Considering the 500 ps delay between pulses, the twofold pulse spread over 1 ns total duration. For the first and second electric pulses, durations of 270 and 253 ps were produced, respectively. Their rise times was similar i.e., 70 ps. The output voltage and temporal gap between the two pulses can be controlled by switching the efficiency and the delay between the optical beams. The output spectrum of the resulting twofold pulse is also presented on Fig. 4(f), showing periodic peaks inversely proportional to the delay between the two voltage pulses. Temporal profile and corresponding spectra of unipolar pulses vary as a function of the laser triggering energy and output voltage as previously demonstrated [11]. For an energy equal to 20 µJ, a unipolar pulse was also generated with 1.68 kV maximum amplitude, 105 ps duration and 60 ps rise time (data not shown).

B. Microwave Spectroscopy

In this section, the spectrum of the dielectric resonator located in the TEM cell obtained using the implemented spectroscopy setup is compared to numerical and experimental $|S_{21}|$ scattering parameters. Results show that the spectrum of the signal obtained by single-shot microwave spectroscopy is similar to the measured transmission coefficient $|S_{21}|$ (Fig. 5). Five main resonance peaks are observed at the frequency values of 1.8, 2.2, 2.4, 2.9 and 3.8 GHz. As each material has its specific resonances, these measurements allow identification of the main components of the resonator.

Experimental and numerical results of the transmission coefficient $|S_{21}|$ of the TEM cell containing the resonator are also presented in Fig. 5. Results agree with the frequency resonance peaks observed when using microwave spectroscopy. Note that the slight shift between the resonances at 1.8 and 3.9 GHz can be due to the differences between modelled and measured structures (geometry, electrical characteristics). However, the resonance peaks, enabling the identification of the resonator, are identical for the two measurement methodologies and for numerical calculations.

V. CONCLUSION

In this paper, we designed and characterized an ultrashort electric pulses generator coupled with an ultrafast microwave spectroscopy system. Unipolar, bipolar, and successive unipolar pulses were generated by tuning the incident optical energy and the temporal delay between the PCSSs activation. The generated pulses had durations of 105, 333, and 253 ps with corresponding output maximum voltage values of 1.68, 1.6, and 0.67 for unipolar, bipolar, and successive unipolar pulses, respectively.

The generator coupling with an ultrafast microwave spectroscopy system allowed to obtain the resonances of a passive dielectric resonator at frequencies up to 5 GHz. The resonance peaks measured with the microwave spectroscopy device were compared to both experimental and numerical |S21| parameters of the TEM cell containing the resonator. Similar resonance peaks were obtained for the three approaches demonstrating the accuracy of the developed single-shot microwave spectroscopy technique. Future perspectives include the possibility to couple the psPEF generator with a fast-non-linear imaging technique, e.g., M-CARS, for real-time synchronized bioelectric investigations and ultrafast imaging.

AKNOWLEDGMENT

Region Nouvelle-Aquitaine (grant AAPR2019-00031603) and ANR (grant ANR-18-CE08-0016).

FIGURES LEGEND

Fig. 1. Experimental setup of the simultaneous pulse generation and microwave spectroscopy.

Fig. 2. 3D model of the TEM cell with the resonator.

Fig. 3. (a) Temporal and (b) spectral bipolar pulse profiles generated by a FW generator excited with 350 fs pulses.

Fig. 4. (a) Experimental setup used for twofold pulses with a 2 cm transmission line and 4 kV input voltage. Electric pulse activated by (b) F1a, (c) F1b, and (d) F2 optical beams; (e) twofold electric pulse obtained through coherent combination of F1a, F1b, and F2; (f) spectrum of the twofold pulse.

Fig.5. Measured and numerically calculated $|S_{21}|$ values of the TEM cell accommodating the resonator compared to measurements through microwave spectroscopy using the generator connected to the TEM cell.

REFERENCES

[1] K. H. Schoenbach, R. Joshi, J. Kolb, S. Buescher, and S. Beebe, "Subcellular effects of nanosecond electrical pulses," in *26th Annual International Conference of the IEEE Engineering in Medicine and Biology Society, 2004. IEMBS '04*, Sep. 2004, vol. 2, pp. 5447–5450. doi: 10.1109/IEMBS.2004.1404522.

[2] S. J. Beebe, "Effects of usEPs on Plasma Membranes—Pores, Channels, and Repair," in *Ultrashort Electric Pulse Effects in Biology and Medicine*, S. J. Beebe, R. Joshi, K. H. Schoenbach, and S. Xiao, Eds. Singapore: Springer, 2021, pp. 33–75. doi: 10.1007/978-981-10-5113-5_2.

[3] P. Butkus, A. Murauskas, S. Tolvaišienė, and V. Novickij, "Concepts and Capabilities of In-House Built Nanosecond Pulsed Electric Field (nsPEF) Generators for Electroporation: State of Art," *Applied Sciences*, vol. 10, no. 12, Art. no. 12, Jan. 2020, doi: 10.3390/app10124244.

[4] P. Leveque, R. O'Connor, and D. Arnaud-Cormos, "Measurement and Characterization of Exposure Systems for High-Frequency, Ultrashort Pulses," in *Handbook of Electroporation*, D. Miklavčič, Ed. Cham: Springer International Publishing, 2017, pp. 813–836. doi: 10.1007/978-3-319-32886-7_207.

[5] S. Kohler, V. Couderc, R. P. O'Connor, D. Arnaud-Cormos, and P. Leveque, "A versatile high voltage nano- and sub-nanosecond pulse generator," *IEEE Transactions on Dielectrics and Electrical Insulation*, vol. 20, no. 4, pp. 1201–1208, Aug. 2013.

[6] J. M. Sanders, A. Kuthi, and M. A. Gundersen, "Optimization and implementation of a solid state high voltage pulse generator that produces fast rising nanosecond pulses," *IEEE Transactions on Dielectrics and Electrical Insulation*, vol. 18, no. 4, pp. 1228–1235, 2011, doi: 10.1109/TDEI.2011.5976120.

[7] M. Nagahama, N. Shimomura, A. Nakagawa, K. Teranishi, Y. Uto, and H. Hori, "In vivo experimental study of nanosecond pulsed electric field effects on solid tumors," *IEEE Transactions on Dielectrics and Electrical Insulation*, vol. 20, no. 4, pp. 1266–1272, 2013, doi: 10.1109/TDEI.2013.6571443.

[8] R. A. Petrella, S. Xiao, and S. Katsuki, "An air core pulse transformer with a linearly integrated primary capacitor bank to achieve ultrafast charging," *IEEE Transactions on Dielectrics and Electrical Insulation*, vol. 23, no. 4, pp. 2443–2449, 2016, doi: 10.1109/TDEI.2016.7556524.

[9] B. Vergne, V. Couderc, and P. Leveque, "A 30-kHz Monocycle Generator Using Linear Photoconductive Switches and a Microchip Laser," *IEEE Photon. Technol. Lett.*, vol. 20, no. 24, pp. 2132–2134, Dec. 2008, doi: 10.1109/LPT.2008.2007132.

[10] S. El Amari *et al.*, "Kilovolt, Nanosecond, and Picosecond Electric Pulse Shaping by Using Optoelectronic Switching," *IEEE Photon. Technol. Lett.*, vol. 22, no. 21, pp. 1577–1579, Nov. 2010, doi: 10.1109/LPT.2010.2073458.

[11] S. El Amari, A. De Angelis, D. Arnaud-Cormos, V. Couderc, and P. Leveque, "Characterization of a Linear Photoconductive Switch Used in Nanosecond Pulsed Electric Field Generator," *IEEE Photonics Technology Letters*, vol. 23, no. 11, pp. 673–675, Jun. 2011, doi: 10.1109/LPT.2011.2122251.

[12] D. Arnaud-Cormos, V. Couderc, and P. Leveque, "Photoconductive Switching for Pulsed High-Voltage Generators," in *Handbook of Electroporation*, D. Miklavčič, Ed. Cham: Springer International Publishing, 2017, pp. 837–857. doi: 10.1007/978-3-319-32886-7_208.

[13] A. Azan *et al.*, "Demonstration of the Protein Involvement in Cell Electropermeabilization using Confocal Raman Microspectroscopy," *Sci Rep*, vol. 7, no. 1, Art. no. 1, Jan. 2017, doi: 10.1038/srep40448.

[14] E. Capitaine *et al.*, "Coherent anti-Stokes Raman scattering under electric field stimulation," *Physical Review B: Condensed Matter and Materials Physics (1998-2015)*, vol. 94, no. 24, p. 245136, 2016, doi: 10.1103/PhysRevB.94.245136.

[15] P. Leproux, V. Couderc, A. de Angelis, M. Okuno, H. Kano, and H. Hamaguchi, "New opportunities offered by compact sub-nanosecond supercontinuum sources in ultra-broadband multiplex CARS microspectroscopy," *Journal of Raman Spectroscopy*, vol. 42, no. 10, pp. 1871–1874, 2011, doi: 10.1002/jrs.2995.

[16] Z. A. Levine and P. T. Vernier, "Life cycle of an electropore: field-dependent and field-independent steps in pore creation and annihilation," *J Membr Biol*, vol. 236, no. 1, pp. 27–36, Jul. 2010, doi: 10.1007/s00232-010-9277-y.

[17] M. Tarek, "Membrane Electroporation: A Molecular Dynamics Simulation," *Biophysical Journal*, vol. 88, no. 6, pp. 4045–4053, Jun. 2005, doi: 10.1529/biophysj.104.050617.

[18] M. Soueid *et al.*, "Electromagnetic Analysis of an Aperture Modified TEM Cell Including an Ito Layer for Real-Time Observation of Biological Cells Exposed to Microwaves," *Progress In Electromagnetics Research*, vol. 149, pp. 193–204, 2014, doi: 10.2528/PIER14053108.

[19] D. Petitprez and G. Wlodarczak, "Microwave Fourier transform spectrometers: a powerful tool for the spectroscopy in the XXIst century," *Comptes Rendus Physique*, vol. 5, no. 2, pp. 231–238, Mar. 2004, doi: 10.1016/j.crhy.2004.01.019.

[20] T. Ozturk, "Classification of measured unsafe liquids using microwave spectroscopy system by multivariate data analysis techniques," *Journal of Hazardous Materials*, vol. 363, pp. 309–315, Feb. 2019, doi: 10.1016/j.jhazmat.2018.09.092.

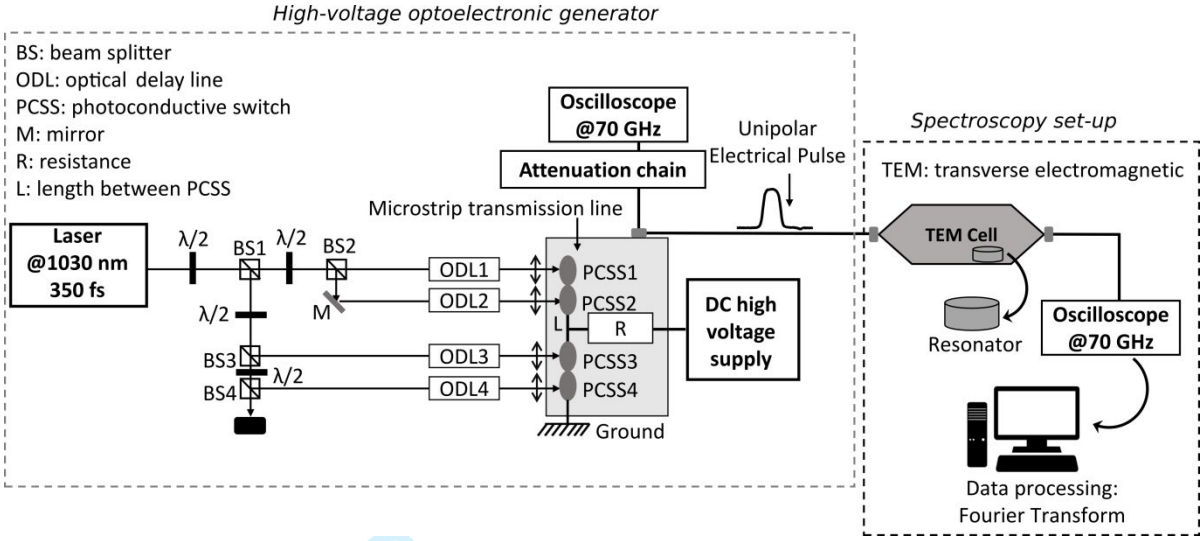
High-voltage optoelectronic generator
BS: beam splitter
ODL: optical delay line
PCSS: photoconductive switch
M: mirror
R: resistance
L: length between PCSS
Oscilloscope @70 GHz
Attenuation chain
Unipolar Electrical Pulse
Microstrip transmission line
Laser @1030 nm 350 fs
λ/2
BS1
BS2
M
BS3
BS4
ODL1
ODL2
ODL3
ODL4
PCSS1
PCSS2
PCSS3
PCSS4
L
R
DC high voltage supply
Ground
Spectroscopy set-up
TEM: transverse electromagnetic
TEM Cell
Resonator
Oscilloscope @70 GHz
Data processing: Fourier Transform

Fig. 1.

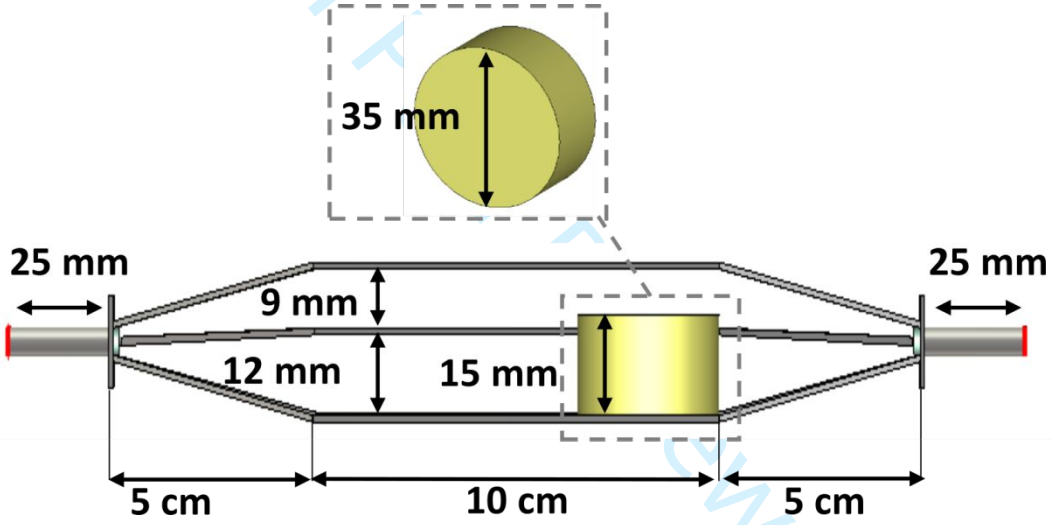
35 mm
25 mm
25 mm
9 mm
12 mm
15 mm
5 cm
10 cm
5 cm

Fig. 2.

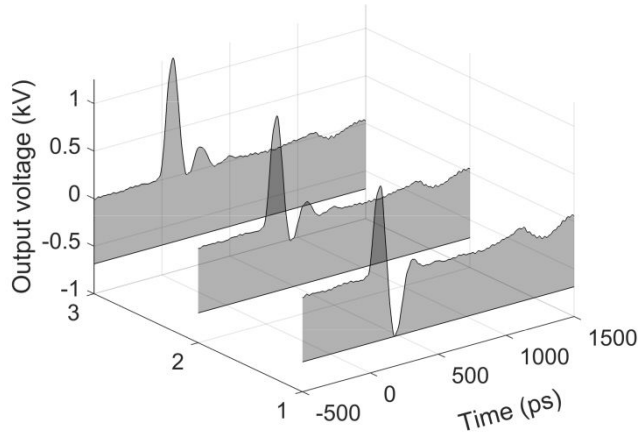
Output voltage (kV)
1
0.5
0
-0.5
-1
3
2
1
-500
0
500
1000
1500
Time (ps)

(a)

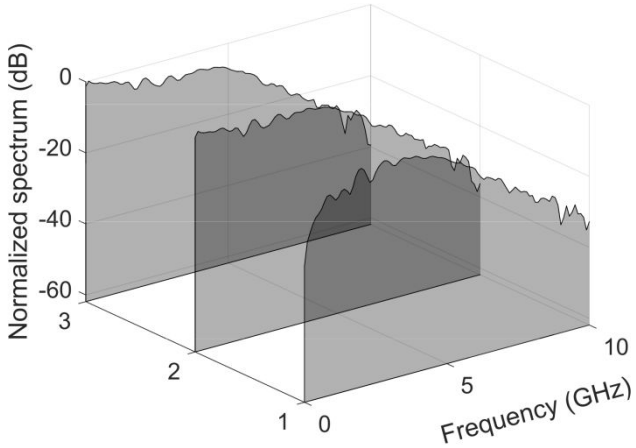
Normalized spectrum (dB)
0
-20
-40
-60
3
2
1
0
5
10
Frequency (GHz)

(b)

Fig. 3.

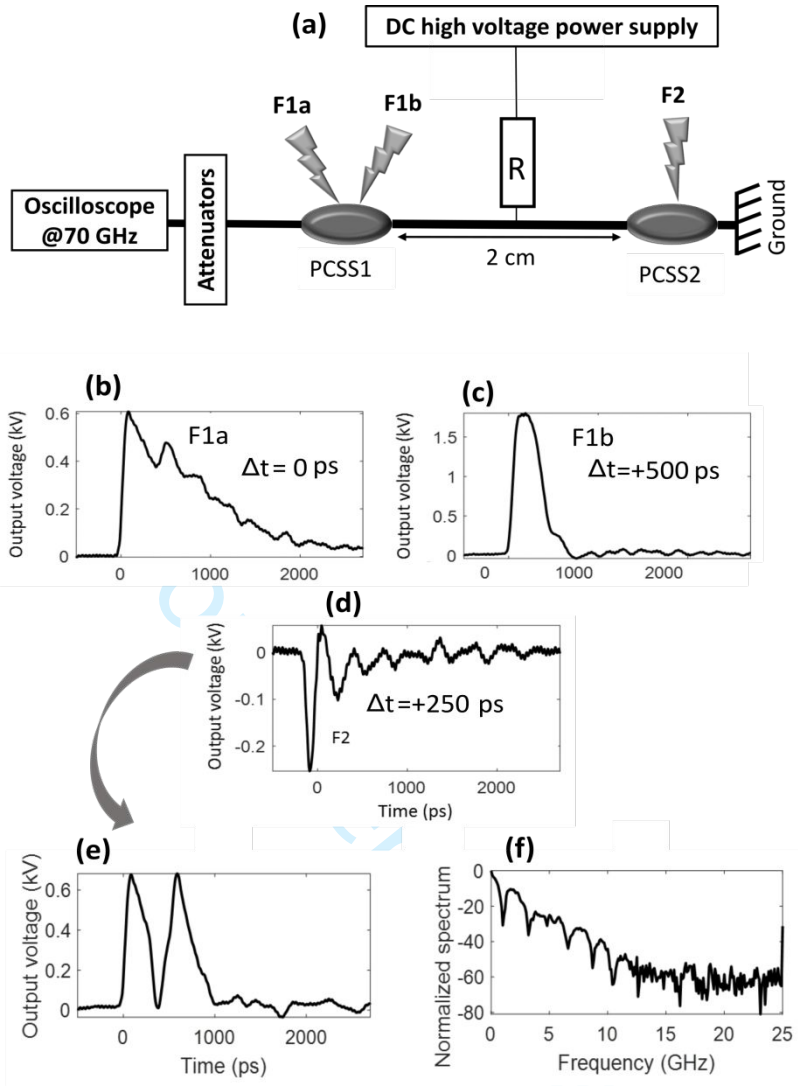
(a)
DC high voltage power supply
F1a
F1b
F2
R
Oscilloscope @70 GHz
Attenuators
PCSS1
2 cm
PCSS2
Ground
(b)
F1a
Δt = 0 ps
Output voltage (kV)
(c)
F1b
Δt=+500 ps
Output voltage (kV)
(d)
Δt=+250 ps
F2
Output voltage (kV)
Time (ps)
(e)
Output voltage (kV)
Time (ps)
(f)
Normalized spectrum
Frequency (GHz)

Fig. 4.

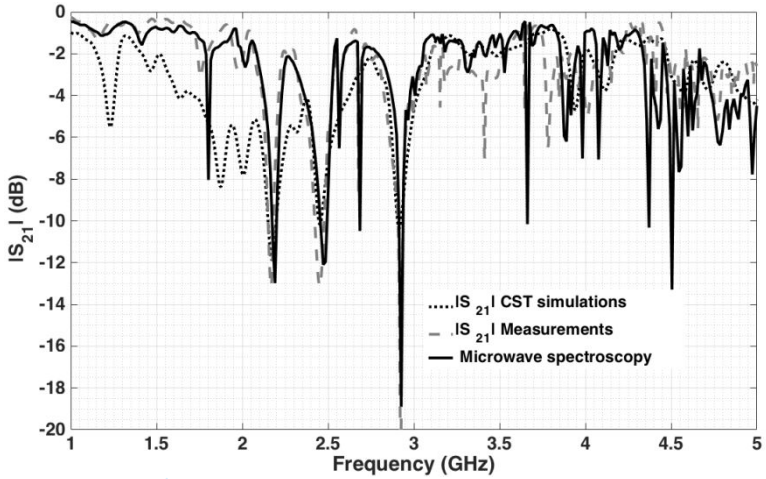

Fig. 5.